Journal of Materials Chemistry A

PAPER

View Article Online
View Journal | View Issue

Check for updates

Cite this: J. Mater. Chem. A, 2019, 7, 13585

Pore environment engineering in metal–organic frameworks for efficient ethane/ethylene separation†

Xun Wang,‡[ab] Zheng Niu,‡[b] Abdullah M. Al-Enizi,[c] Ayman Nafady,[cd] Yufang Wu,[a] Briana Aguila, [b] Gaurav Verma,[b] Lukasz Wojtas,[b] Yu-Sheng Chen,[e] Zhong Li*[a] and Shengqian Ma *[b]

Received 15th March 2019
Accepted 6th May 2019

DOI: 10.1039/c9ta02822f

rsc.li/materials-a

Selective adsorption of trace amounts of C_2H_6 from bulk C_2H_4 is a significantly important and extremely challenging task in industry, which requires an adsorbent with specific pore properties. Herein, we describe a strategy for adjusting the pore environment of metal–organic frameworks (MOFs) by introducing different amounts of methyl groups in the channel to enhance the guest–host interaction between C_2H_6 and the framework. To prove this concept, 2,3,5,6-tetramethylterephthalic acid (TMBDC) was deliberately added to a microporous MOF, Ni(BDC)(DABCO)$_{0.5}$, affording a series of mixed-ligand materials, Ni(BDC)$_{1-x}$(TMBDC)$_x$(DABCO)$_{0.5}$ ($x = 0$, 0.2, 0.45, 0.71, 1), having different pore environments. Significantly, these mixed-ligand materials demonstrated improved performance in terms of the adsorption capacity of C_2H_6 and C_2H_4 with an unprecedented C_2H_6 uptake of 2.21 mmol g^{-1} for Ni(TMBDC)(DABCO)$_{0.5}$ at 0.0625 bar and 298 K. With the best theoretical C_2H_6/C_2H_4 selectivity predicted by IAST, Ni(TMBDC)(DABCO)$_{0.5}$ exhibited effective separation of C_2H_6/C_2H_4 (1/15, v/v) and great recyclability in five consecutive adsorption/desorption cycles throughout the breakthrough experiment.

Introduction

As the most important raw material for manufacturing plastics, ethylene (C_2H_4) is primarily obtained *via* steam cracking and thermal decomposition of ethane (C_2H_6).[1] The separation of C_2H_4/C_2H_6 mixtures becomes a challenging issue at the large scale because of their similar molecular sizes and volatilities.[2] In industry, ethylene is separated from ethane through cryogenic distillation at low temperature (183–258 K) and high pressure (7–28 bar), making it an extremely energy exhaustive process.[1,2] Therefore, separation approaches that have low cost and energy-saving characteristics are highly desirable in industry. Among several new technologies, adsorptive separation has attracted extensive interest due to its operational simplicity and ability to afford high product purity.[3–5] The cornerstone of this promising technology is a solid adsorbent with specific properties.

Over the past few decades, metal–organic frameworks (MOFs)[6–13] have been explored as a kind of highly efficient solid adsorbent for gas storage and separation because of their high surface areas, adjustable pore environments, and designable framework structures.[14–25] Research on the separation of ethylene/ethane using MOFs with open metal sites has been widely reported, in which high ethylene uptake capacities and C_2H_4/C_2H_6 selectivities have been achieved.[26–32] Furthermore, π-complexation adsorbents,[33] such as Cu(I)-based sorbents[34,35] and Ag(I)-based sorbents,[36–39] were developed since these materials can form π-complexes with the carbon–carbon double bonds of C_2H_4, resulting in higher ethylene capacities and C_2H_4 selectivities over C_2H_6. Virtually, these materials preferentially adsorb C_2H_4 in C_2H_4/C_2H_6 mixtures owing to the interactions between the open metal sites of the MOFs and C_2H_4 or formation of π-complexes. Such a behavior is expected to consume more energy during desorption because these interactions are stronger than the traditional physisorption.

Practically, the ethylene concentration in the cracked gas feed is much higher than that of ethane ($C_2H_4 : C_2H_6 = 15 : 1$,

[a]School of Chemistry and Chemical Engineering, South China University of Technology, Guangzhou, 510640, China. E-mail: cezhli@scut.edu.cn
[b]Department of Chemistry, University of South Florida, 4202 East Fowler Avenue, Tampa, Florida, 33620, USA. E-mail: sqma@usf.edu; Fax: +1 813-974-3203; Tel: +1 813-974-5217
[c]Department of Chemistry, College of Science, King Saud University, Riyadh 11451, Saudi Arabia
[d]Chemistry Department, Faculty of Science, Sohag University, Sohag 82524, Egypt
[e]ChemMatCARS, Center for Advanced Radiation Sources, The University of Chicago, 9700 South Cass Avenue, Argonne, Illinois 60439, USA

† Electronic supplementary information (ESI) available: Experimental details, TGA curves, ^{1}H NMR data and single-crystal data. CCDC 1879219. For ESI and crystallographic data in CIF or other electronic format see DOI: 10.1039/c9ta02822f

‡ These authors contributed equally to this work.

v/v) and consequently large amounts of adsorbents are required, giving rise to a larger packed-bed column. In this context, it is strategically essential to develop ethane-selective adsorbents for preferential adsorption of trace amounts of C_2H_6 from bulk C_2H_4. Nevertheless, this class of materials has rarely been reported and most of them exhibited poor C_2H_6/C_2H_4 adsorption capacities and/or separation performances.[40–45] Importantly, simulation and experimental results revealed that C_2H_6 interacts more strongly with the material's framework than C_2H_4 owing to the fact that C_2H_6 has more C–H bonds.[41,43–46] Inspired by these endeavors, we propose a strategy for constructing a binding environment in MOFs that favors C_2H_6 over C_2H_4, through adjusting the guest–host interaction between the pores and C_2H_6 molecules as illustrated in Scheme 1.

To prove the above concept, we employed a MOF, Ni(BDC)(DABCO)$_{0.5}$,[41,47,48] (BDC = terephthalic acid, DABCO = 1,4-diazabicyclo[2.2.2]octane) as a prototype host material. Methyl group functionalized pores were constructed by introducing different amounts of the TMBDC ligand (TMBDC = 2,3,5,6-tetramethylterephthalic acid) into the framework of Ni(BDC)(DABCO)$_{0.5}$ through a mixed-ligand strategy, affording a series of MOFs, Ni(BDC)$_{1-x}$(TMBDC)$_x$(DABCO)$_{0.5}$ (x = 0, 0.2, 0.45, 0.71, 1). The obtained MOFs retained a similar framework, yet exhibited varying C_2H_6/C_2H_4 adsorption performances with change in the mole ratio of TMBDC/BDC. The selectivity of C_2H_6/C_2H_4 based on ideal adsorbed solution theory (IAST) using single component experimental adsorption isotherms illustrated that the introduction of a methyl group into a MOF can effectively enhance the C_2H_6/C_2H_4 separation performance. The designed breakthrough experiments confirmed the IAST calculated results, whereas the adsorption/desorption cycling tests implied the robustness and excellent recyclability of the material.

Experimental

Chemicals

All chemical reagents were purchased from commercial sources (Sigma-Aldrich, Alfa, Fisher, Acros, TCI, *etc.*) and used without further purification. 2,3,5,6-tetramethylterephthalic acid (TMBDC) was synthesized according to a procedure reported in the literature with some modification (ESI†).[49]

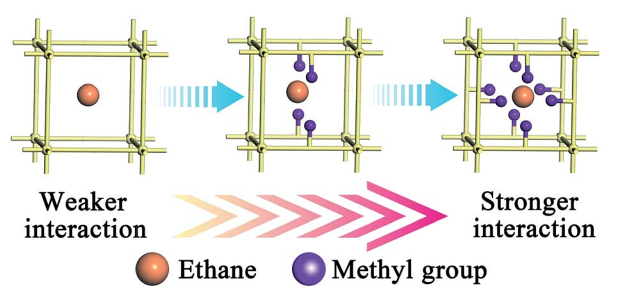

Scheme 1 Schematic illustration of methyl group functionalization in MOF pores to enhance the interaction toward ethane molecule.

Synthesis of Ni(BDC)$_{1-x}$(TMBDC)$_x$(DABCO)$_{0.5}$ (x = 0, 0.2, 0.45, 0.71, 1)

General procedure. A 20 mL vial was charged with Ni(NO$_3$)$_2$·6H$_2$O (0.093 g, 0.32 mmol), DABCO (0.018 g, 0.16 mmol), BDC ligands (TMBDC and/or BDC) and 8 mL DMF. After vigorous stirring, one drop of HNO_3 was added. The mixture was sonicated to get a clear solution and then heated at 120 °C for 48 h to afford green crystals. The crystals were collected by filtration and soaked in DMF to remove any residual reactants and then ethanol to exchange the DMF. The obtained Ni(BDC)$_{1-x}$(TMBDC)$_x$(DABCO)$_{0.5}$ were kept in ethanol until use. The exact ratio of TMBDC/BDC was determined by ^{1}H NMR after decomposing the MOFs using HCl solution (ESI, Fig. S5–S9†).

Synthesis of Ni(BDC)$_{0.8}$(TMBDC)$_{0.2}$(DABCO)$_{0.5}$. A 20 mL vial was filled with Ni(NO$_3$)$_2$·6H$_2$O (0.093 g, 0.32 mmol), DABCO (0.018 g, 0.16 mmol), TMBDC (0.014 g, 0.06 mmol), BDC (0.04 g, 0.24 mmol) and 8 mL DMF. After being heated up to 120 °C for 48 h and purified with DMF and ethanol, Ni(BDC)$_{0.8}$(TMBDC)$_{0.2}$(DABCO)$_{0.5}$ was obtained (yield: 86% based on DABCO). Elemental analysis of $C_{11.8}H_{13.6}NO_4Ni$, calcd (%) C, 48.47; H, 4.66; N, 4.66. Found: C, 48.57; H, 4.78; N, 4.56. FTIR (cm^{-1}): 2959 (br), 1613 (m), 1511 (s), 1382 (s), 1229 (w), 1055 (m), 1022 (m).

Synthesis of Ni(BDC)$_{0.55}$(TMBDC)$_{0.45}$(DABCO)$_{0.5}$. A 20 mL vial was filled with Ni(NO$_3$)$_2$·6H$_2$O (0.093 g, 0.32 mmol), DABCO (0.018 g, 0.16 mmol), TMBDC (0.034 g, 0.15 mmol), BDC (0.025 g, 0.15 mmol) and 8 mL DMF. After being heated up to 120 °C for 48 h and purified with DMF and ethanol, Ni(BDC)$_{0.55}$(TMBDC)$_{0.45}$(DABCO)$_{0.5}$ was obtained (yield: 80% based on DABCO). Elemental analysis of $C_{12.8}H_{15.6}NO_4Ni$, calcd (%) C, 50.17; H, 5.10; N, 4.57. Found: C, 49.87; H, 5.46; N, 4.46. FTIR (cm^{-1}): 2933 (br), 1603 (m), 1548 (w), 1392 (s), 1230 (s), 1053 (m), 1016 (m).

Synthesis of Ni(BDC)$_{0.29}$(TMBDC)$_{0.71}$(DABCO)$_{0.5}$. A 20 mL vial was filed with Ni(NO$_3$)$_2$·6H$_2$O (0.093 g, 0.32 mmol), DABCO (0.018 g, 0.16 mmol), TMBDC (0.054 g, 0.24 mmol), BDC (0.01 g, 0.06 mmol) and 8 mL DMF. After being heated up to 120 °C for 48 h and purified with DMF and ethanol, Ni(BDC)$_{0.29}$(TMBDC)$_{0.71}$(DABCO)$_{0.5}$ was obtained (yield: 73% based on DABCO). Elemental analysis of $C_{13.84}H_{17.68}NO_4Ni$, calcd (%) C, 51.78; H, 5.51; N, 4.36. Found: C, 51.53; H, 5.90; N, 4.29. FTIR (cm^{-1}): 2929 (br), 1601 (m), 1538 (m), 1441 (s), 1376 (s), 1235 (s), 1061 (m), 1016 (m).

Synthesis of Ni(TMBDC)(DABCO)$_{0.5}$. A 20 mL vial was filled with Ni(NO$_3$)$_2$·6H$_2$O (0.093 g, 0.32 mmol), DABCO (0.018 g, 0.16 mmol), TMBDC (0.067 g, 0.3 mmol) and 8 mL DMF. After being heated up to 120 °C for 48 h and purified with DMF and ethanol, the Ni(TMBDC)(DABCO)$_{0.5}$ was obtained (yield: 68% based on DABCO). Elemental analysis of $C_{15}H_{20}NO_4Ni$, calcd (%) C, 53.41; H, 5.93; N, 4.15. Found: C, 53.16; H, 6.28; N, 4.19. FTIR (cm^{-1}): 2943 (br), 1603 (m), 1596 (s), 1445 (s), 1376 (s), 1230 (s), 1057 (m), 1010 (m).

Synthesis of Ni(BDC)(DABCO)$_{0.5}$. For comparison, Ni(BDC)(DABCO)$_{0.5}$ was prepared according to procedures described elsewhere.[41,47,48]

Characterization

N_2 adsorption–desorption isotherms were measured at 77 K using a liquid N_2 bath. The surface area was calculated using the Brunauer–Emmett–Teller equation in the range $P/P_0 = 0.05$–0.35, while the pore size distribution was calculated by the DFT method. All samples were degassed at 120 °C for 6 h before analysis. Powder X-ray diffraction (PXRD) were performed on a Bruker AXS D8 Advance using Cu Kα ($\lambda = 1.5406$ Å) radiation. FT-IR data were recorded on a PerkinElmer Spectrum Two. TGA curves were obtained using a NETZSCH STA 449F3 simultaneous thermal analyzer (NETZSCH, Germany). ^{1}H NMR spectra were recorded on a Unity Inova 400 Spectrometer (400 MHz).

Gas adsorption isotherms

C_2H_6 and C_2H_4 adsorption isotherms were collected on a 3Flex Surface Characterization Analyzer (Micromeritics, USA). Before each measurement, the samples were degassed at 120 °C under vacuum for 6 h.

Breakthrough experiments

The breakthrough curves of the gas mixture C_2H_6/C_2H_4 (1 : 15, v/v) were collected on a self-assembly experimental apparatus (Fig. S2†). Breakthrough experiments were carried out at 298 K on a gas chromatography apparatus (GC-9560, Shanghai Huaai), equipped with a 2 m long Al_2O_3-packed column with an FID detector. Typically, ∼200 mg pre-degassed sample was packed into a stainless steel column with inner dimensions of Φ 6 × 275 mm. The carrier gas was N_2 having a flow rate of 45 mL min^{-1}, and the flow rate of the C_2H_6/C_2H_4 gas mixture was controlled at 1 mL min^{-1} by using a mass flow controller (FMA-A200, America). For the consecutive adsorption/desorption cycling tests, the sample packed column was regenerated by purging He at a rate of 30 mL min^{-1} at 100 °C for 20 min. After that the gas flow was switched to the C_2H_6/C_2H_4 mixture for the next cycle.

Results and discussion

Characterization of the materials

Solvothermal reaction of terephthalic acid (H_2BDC), 2,3,5,6-tetramethylterephthalic acid (TMBDC), and 1,4-diazabicyclo[2.2.2]octane (DABCO) with $Ni(NO_3)_2\cdot 6H_2O$ in DMF at 120 °C yielded green rod-shaped crystals of $Ni(BDC)_{1-x}(TMBDC)_x(DABCO)_{0.5}$ ($x = 0.2$, 0.45, 0.71, 1). Single crystal X-ray diffraction measurements were employed to analyze the structures of the MOFs, and the results revealed that all mixed-ligand samples crystallized in the *P*4/*mmm* space group (Fig. 1a). The structure of $Ni(TMBDC)(DABCO)_{0.5}$ is presented and discussed, since all of them are isostructural. As shown in Fig. 1, each nickel paddlewheel is connected with four linear linkers of TMBDC^{2-} to form two-dimensional layers, while the DABCO molecules coordinate at the vertex of the nickel paddlewheels as the pillar to bridge the layers, thus affording a 3D framework (Fig. 1b). Assuming the nickel paddlewheel to be the 6-connected nodes and the ligands as linkers, $Ni(TMBDC)(DABCO)_{0.5}$ displays a 6-coordinated network with the topology of ***pcu*** (Fig. 1c). The

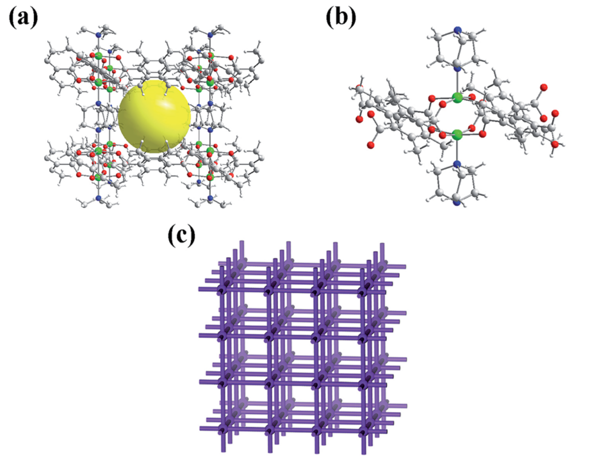

Fig. 1 (a) The primary cavity of $Ni(TMBDC)(DABCO)_{0.5}$; (b) the connection of one nickel paddlewheel and linkers; (c) ***pcu*** topology of $Ni(TMBDC)(DABCO)_{0.5}$ (green, nickel; grey, carbon; blue, nitrogen; red, oxygen; white, hydrogen).

primary cavity of $Ni(BDC)_{1-x}(TMBDC)_x(DABCO)_{0.5}$ ($x = 0.2$, 0.45, 0.71, 1) is constructed using eight nickel paddlewheels, eight BDC^{2-} ligands, and four DABCO pillared ligands, exhibiting a cubic shaped cavity suitable to fit a sphere with a diameter of 6.5–8.7 Å, which increased along with the decrease of the TMBDC/BDC ratio.

The phase purity of the five materials was confirmed by PXRD studies. As shown in Fig. 2a, the series of materials show high crystallinity and purity. The PXRD patterns of $Ni(BDC)(DABCO)_{0.5}$ are in good agreement with those reported in the literature.[41,47,48] $Ni(BDC)_{1-x}(TMBDC)_x(DABCO)_{0.5}$ ($x = 0.2$, 0.45, 0.71, 1) retained the same XRD patterns as those of $Ni(BDC)(DABCO)_{0.5}$, implying that the introduction of the TMBDC ligand did not interrupt the crystal phase purity. The thermal stability of $Ni(BDC)_{1-x}(TMBDC)_x(DABCO)_{0.5}$ ($x = 0$, 0.2,

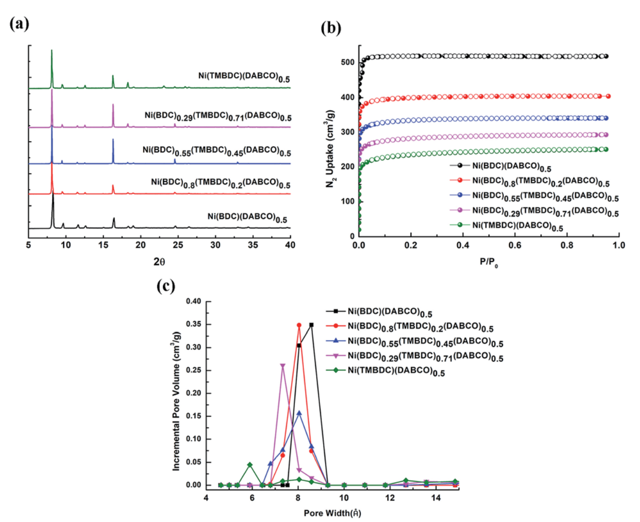

Fig. 2 (a) PXRD patterns, (b) N_2 adsorption–desorption isotherms at 77 K and (c) pore size distributions of $Ni(BDC)_{1-x}(TMBDC)_x(DABCO)_{0.5}$ ($x = 0$, 0.2, 0.45, 0.71, 1).

0.45, 0.71, 1) was studied by thermogravimetric analysis. All TGA curves exhibited a negligible weight loss before 400 °C and great loss (∼65%) after that temperature, which indicated $Ni(BDC)_{1-x}(TMBDC)_x(DABCO)_{0.5}$ ($x = 0, 0.2, 0.45, 0.71, 1$) were thermally stable up to 400 °C (Fig. S2†).

Nitrogen adsorption–desorption isotherms at 77 K were used to investigate the porosity of $Ni(BDC)_{1-x}(TMBDC)_x(DABCO)_{0.5}$ ($x = 0, 0.2, 0.45, 0.71, 1$). As shown in Fig. 2b, all five materials exhibit typical type-I sorption behaviors, suggesting the microporous structure in their frameworks. With the increase of the TMBDC/BDC ratio, the BET surface area and pore volume of $Ni(BDC)_{1-x}(TMBDC)_x(DABCO)_{0.5}$ ($x = 0, 0.2, 0.45, 0.71, 1$) decreases from 2050 $m^2\ g^{-1}$ and 0.80 $cm^3\ g^{-1}$ for $Ni(BDC)(DABCO)_{0.5}$ to 894 $m^2\ g^{-1}$ and 0.39 $cm^3\ g^{-1}$ for $Ni(TMBDC)(DABCO)_{0.5}$, respectively (Table 1). The decrease of both BET surface area and accessible pore volume can be ascribed to the increased number of methyl groups in the framework (Table 1).

Pore size distribution analysis performed by the density functional theory (DFT) method further confirmed the methyl group occupation in the pores. The results showed that with the increase of the TMBDC/BDC ratio, the main pore size distribution is shifted from ∼8.3 Å for $Ni(BDC)(DABCO)_{0.5}$ to ∼5.9 Å for 100% $Ni(TMBDC)(DABCO)_{0.5}$.

Consequently, we have judiciously tuned the pore size and pore environment of the pristine $Ni(BDC)(DABCO)_{0.5}$ by introducing the TMBDC ligand into the framework. Through altering the TMBDC/BDC ratio, mixed-ligand materials, $Ni(BDC)_{1-x}(TMBDC)_x(DABCO)_{0.5}$ ($x = 0, 0.2, 0.45, 0.71, 1$), were successfully synthesized, which is expected to influence the adsorption and separation performances of C_2H_6 and C_2H_4 to obtain desirable C_2H_6/C_2H_4 separation selectivity.

The success of constructing methyl group functionalized pores in the MOFs prompted us to investigate the C_2H_6 and C_2H_4 adsorption performance of $Ni(BDC)_{1-x}(TMBDC)_x(DABCO)_{0.5}$ ($x = 0, 0.2, 0.45, 0.71, 1$). Single component adsorption isotherms of both C_2H_6 and C_2H_4 (Fig. 3, S3–S9†) were measured at 273 K, 298 K and 308 K. As shown in Fig. 3, all of the $Ni(BDC)_{1-x}(TMBDC)_x(DABCO)_{0.5}$ ($x = 0, 0.2, 0.45, 0.71, 1$) exhibited preferential adsorption of C_2H_6 over C_2H_4. The equilibrium uptake of C_2H_6 and C_2H_4 for $Ni(BDC)(DABCO)_{0.5}$ can reach 4.36 mmol g^{-1} and 3.04 mmol g^{-1} at 1 bar, respectively. However, the C_2H_6 and C_2H_4 uptake amounts in the low pressure region (0–0.3 bar) are not high, which are insufficient to address the challenging issue of the industrial separation of C_2H_6 and C_2H_4.

Table 1 BET surface areas and pore volumes of $Ni(BDC)_{1-x}(TMBDC)_x(DABCO)_{0.5}$ ($x = 0, 0.2, 0.45, 0.71, 1$)

Materials	BET surface area ($m^2\ g^{-1}$)	Pore volume ($cm^3\ g^{-1}$)
$Ni(BDC)(DABCO)_{0.5}$	2050	0.80
$Ni(BDC)_{0.8}(TMBDC)_{0.2}(DABCO)_{0.5}$	1556	0.63
$Ni(BDC)_{0.55}(TMBDC)_{0.45}(DABCO)_{0.5}$	1294	0.53
$Ni(BDC)_{0.29}(TMBDC)_{0.71}(DABCO)_{0.5}$	1084	0.45
$Ni(TMBDC)(DABCO)_{0.5}$	894	0.39

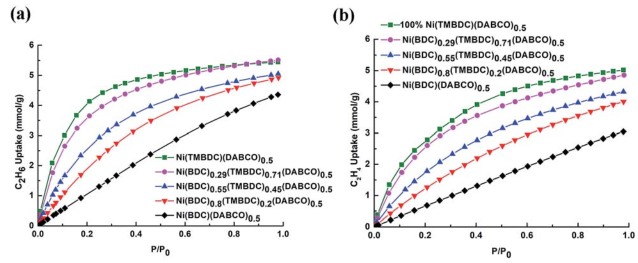

Fig. 3 (a) C_2H_6 and (b) C_2H_4 adsorption isotherms of $Ni(BDC)_{1-x}(TMBDC)_x(DABCO)_{0.5}$ ($x = 0, 0.2, 0.45, 0.71, 1$) at 298 K.

When the concentration of the TMBDC ligand increases, $Ni(BDC)_{1-x}(TMBDC)_x(DABCO)_{0.5}$ ($x = 0.2, 0.45, 0.71, 1$) take up an increasing amount of both ethane and ethylene at 1 bar as well as in the low pressure region (0–0.3 bar). The equilibrium uptake of C_2H_6 and C_2H_4 for $Ni(TMBDC)(DABCO)_{0.5}$ reached 5.45 mmol g^{-1} and 5.02 mmol g^{-1} at 1 bar, respectively, which are comparable with the previously reported values of other materials.[27,28,45,50–52] However, the high C_2H_6 uptakes in the low pressure region make these materials promising for the challenging separation of trace amounts of C_2H_6 from bulk C_2H_4. Given the low concentration of ethane ($C_2H_6 : C_2H_4 = 1 : 15$, v/v) in the industrial cracked gas feed, the gas uptake at 0.0625 bar ($P/P_0 = 0.0625$) should be given more attention. As shown in Fig. 3a, $Ni(TMBDC)(DABCO)_{0.5}$ exhibits an unprecedented C_2H_6 uptake of 2.21 mmol g^{-1} at 0.0625 bar, which is higher than the 1.47 mmol g^{-1} (35 $cm^3\ g^{-1}$) for MAF-49,[42] 2 mmol g^{-1} for $Fe_2(dobdc)$ (318 K),[27] and 0.8 mmol g^{-1} for Cu–BTC (295 K).[51] The higher equilibrium uptake and low-pressure uptake of C_2H_6 and C_2H_4 for $Ni(BDC)_{1-x}(TMBDC)_x(DABCO)_{0.5}$ ($x = 0.2, 0.45, 0.71, 1$) should be ascribed to the introduction of the TMBDC ligand. In principle, as the ratio of TMBDC/BDC increases, the amount of methyl groups from the TMBDC ligand increases, which leads to a stronger interaction toward the gas molecules. C_2H_6 molecules, which have more C–H bonds, are expected to induce stronger interaction with the methyl groups in the MOF than C_2H_4, thereby leading to more preferential adsorption of C_2H_6 in $Ni(BDC)_{1-x}(TMBDC)_x(DABCO)_{0.5}$ ($x = 0.2, 0.45, 0.71, 1$).

In order to assess the potential of $Ni(BDC)_{1-x}(TMBDC)_x(DABCO)_{0.5}$ ($x = 0.2, 0.45, 0.71, 1$) for C_2H_6/C_2H_4 separation, ideal adsorbed solution theory (IAST) was used to predict the C_2H_6/C_2H_4 (1 : 15 v/v) selectivity for all $Ni(BDC)_{1-x}(TMBDC)_x(DABCO)_{0.5}$ ($x = 0, 0.2, 0.45, 0.71, 1$). Before IAST calculations, C_2H_6 and C_2H_4 adsorption isotherms at 298 K were fitted using the dual-site Langmuir-Freundlich (DSLF) model (ESI†). As shown in Fig. 4a, the IAST selectivity of pristine $Ni(BDC)(DABCO)_{0.5}$ is 1.619 at 298 K and 100 kPa. As the ratio of TMBDC/BDC is increased, the selectivity of $Ni(BDC)_{1-x}(TMBDC)_x(DABCO)_{0.5}$ ($x = 0.2, 0.45, 0.71, 1$) increases and reaches up to 1.985 for $Ni(TMBDC)(DABCO)_{0.5}$ at 100 kPa, indicating that it exhibits the best performance for C_2H_6/C_2H_4 separation among the five materials. The interaction between gas molecules and the host framework was evaluated by isosteric heat, Q_{st}, which is calculated using the Clausius–Clapeyron equation (ESI†). The obtained Q_{st} of C_2H_6 is slightly higher than that of C_2H_4, further confirming the preferential adsorption

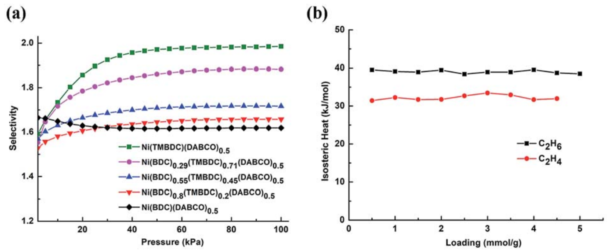

Fig. 4 (a) IAST selectivities of C_2H_6/C_2H_4 (1 : 15) on Ni(BDC)$_{1-x}$(TMBDC)$_x$(DABCO)$_{0.5}$ ($x = 0$, 0.2, 0.45, 0.71, 1) and (b) isosteric heats of C_2H_6 and C_2H_4 adsorption on Ni(TMBDC)(DABCO)$_{0.5}$ at 298 K.

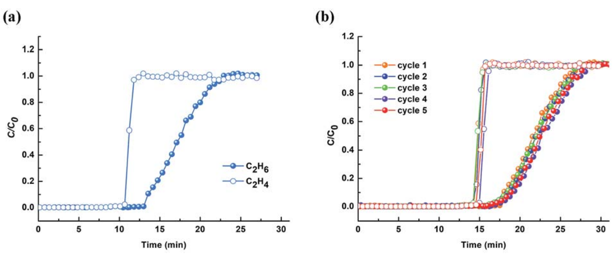

Fig. 5 Breakthrough curves of C_2H_6/C_2H_4 (1 : 15) in a column packed with Ni(TMBDC)(DABCO)$_{0.5}$ at 298 K (a) in a single run and (b) five consecutive adsorption–desorption cycles.

of Ni(TMBDC)(DABCO)$_{0.5}$ toward C_2H_6. Additionally, the Q_{st} values of C_2H_6 in Ni(TMBDC)(DABCO)$_{0.5}$ are ~39 kJ mol^{-1}, which are higher than the reported values including those of Ni(BDC)(DABCO)$_{0.5}$,[41] IRMOF-8,[50] and MAF-3,[42] illustrating a strong guest–host interaction between the framework of Ni(TMBDC)(DABCO)$_{0.5}$ and C_2H_6 molecules. Based on the outstanding IAST calculation results, Ni(TMBDC)(DABCO)$_{0.5}$ was chosen for further investigations.

To explore the dynamic separation of Ni(TMBDC)(DABCO)$_{0.5}$ for the C_2H_6/C_2H_4 mixture, a breakthrough experiment was undertaken, in which the simulated cracked gas feed of C_2H_6/C_2H_4 (1/15, v/v) was used. As shown in Fig. 5a, clean and sharp separation of C_2H_6 and C_2H_4 was observed. The initial outlet effluent gas contains only C_2H_4 with high purity (>99.9%), indicating the efficient separation for the C_2H_6/C_2H_4 mixture when Ni(TMBDC)(DABCO)$_{0.5}$ is used as the adsorbent in the packed column. The recycle test of Ni(TMBDC)(DABCO)$_{0.5}$ was evaluated in the breakthrough apparatus. Fig. 5b shows the breakthrough curves of five consecutive adsorption–desorption cycles in a column packed with Ni(TMBDC)(DABCO)$_{0.5}$. In each cycle, the material was regenerated completely within 20 min, showing remarkable recyclability and enhanced stability in capacity. It should be noted that the Ni(TMBDC)(DABCO)$_{0.5}$ packed column was regenerated without vacuuming, making it feasible for industrial applications.

Conclusions

In summary, a series of Ni(BDC)$_{1-x}$(TMBDC)$_x$(DABCO)$_{0.5}$ ($x = 0.2$, 0.45, 0.71, 1) with controllable methyl group functionalized pores have been successfully constructed for C_2H_6/C_2H_4 separation. The series of MOFs exhibit similar frameworks but different pore environments. Owing to the adjustment of the methyl groups in the framework, Ni(BDC)$_{1-x}$(TMBDC)$_x$(DABCO)$_{0.5}$ ($x = 0$, 0.2, 0.45, 0.71, 1) show different guest–host interactions toward C_2H_6 and C_2H_4 than the pristine material, leading to different adsorption capacities for both C_2H_6 and C_2H_4. Containing more C–H bonds, the adsorption of C_2H_6 is highly favoured in these mixed-ligand materials and an unprecedented C_2H_6 capacity of 2.21 mmol g^{-1} at 0.0625 bar was obtained for Ni(TMBDC)(DABCO)$_{0.5}$. With the best IAST selectivity of 1.985 and a high Q_{st} of 35 kJ mol^{-1} for C_2H_6, Ni(TMBDC)(DABCO)$_{0.5}$ was selected for the breakthrough experiment and recyclability test, which showed great potential for C_2H_6/C_2H_4 (1 : 15, v/v) separation. Significantly, this pore environment engineering approach is most likely to facilitate the design of other novel MOF materials for other important gas separations.

Author contribution

X. W., Z. L., and S. M. conceived the research and designed the experiments; X. W. and Z. N. conducted the experiments of MOF synthesis and gas sorption measurements; G. V., L. W., and Y. S. C. performed the SCXRD studies; all the authors participated in the data discussion and writing of the manuscript.

Conflicts of interest

There are no conflicts to declare.

Acknowledgements

The authors acknowledge the China Scholarship Council (201606150020), the Key Program of the National Natural Science Foundation of China (No. 21436005), the Guangdong Province Science and Technology Project (No. 2016A020221006), the United States National Science Foundation (DMR-1352065) and the University of South Florida for financial support of this work. Single crystal diffraction data were collected at Argonne National Laboratory, Advanced Photon Source, Beamline 15-ID-B of ChemMatCARS, which is principally supported by the Divisions of Chemistry (CHE) and Materials Research (DMR), National Science Foundation, under grant number NSF/CHE-1346572. The use of the PILATUS3 X CdTe 1M detector is supported by the National Science Foundation under the grant number NSF/DMR-1531283. The use of the Advanced Photon Source, an Office of Science User Facility operated for the U.S. Department of Energy (DOE) Office of Science by Argonne National Laboratory, was supported by the U.S. DOE under Contract No. DE-AC02-06CH11357. The authors also extend their appreciation to the Distinguished Scientist Fellowship Program (DSFP) at King Saud University for partial funding of this work.

Notes and references

1 S. Matar and L. F. Hatch, *Chemistry of Petrochemical Processes*, Gulf Publishing Company, 2nd edn, 2001.
2 T. Ren, M. Patel and K. Blok, *Energy*, 2006, **31**, 425.
3 D. S. Sholl and R. P. Lively, *Nature*, 2016, **532**, 435.
4 D. M. Ruthven and S. C. Reyes, *Microporous Mesoporous Mater.*, 2007, **104**, 59.
5 H. Jårvelin and J. R. Fair, *Ind. Eng. Chem. Res.*, 1993, **32**, 2201.
6 P. Kumar, K.-H. Kim, E. E. Kwon and J. E. Szulejko, *J. Mater. Chem. A*, 2016, **4**, 345.
7 H.-C. Zhou, J. R. Long and O. M. Yaghi, *Chem. Rev.*, 2012, **112**, 673.
8 H. Furukawa, K. E. Cordova, M. O'Keeffe and O. M. Yaghi, *Science*, 2013, **341**, 1230444.
9 H.-C. Zhou and S. Kitagawa, *Chem. Soc. Rev.*, 2014, **43**, 5415.
10 J. Jiang, Y. Zhao and O. M. Yaghi, *J. Am. Chem. Soc.*, 2016, **138**, 3255.
11 F. Zare Karizi, M. Joharian and A. Morsali, *J. Mater. Chem. A*, 2018, **6**, 19288.
12 Y. Cui, B. Li, B. Chen and G. Qian, *Acc. Chem. Res.*, 2016, **49**, 483.
13 B. Li, H.-M. Wen, G. Qian, B. Chen, *et al.*, *Adv. Mater.*, 2016, **28**, 8819.
14 M. P. Suh, H. J. Park, T. K. Prasad and D. W. Lim, *Chem. Rev.*, 2012, **112**, 782.
15 X. Zhao, Y. Wang, D.-S. Li, X. Bu and P. Feng, *Adv. Mater.*, 2018, **30**, 1705189.
16 A. Cadiau, K. Adil, P. M. Bhatt, Y. Belmabkhout and M. Eddaoudi, *Science*, 2016, **353**, 137.
17 J.-R. Li, J. Sculley and H.-C. Zhou, *Chem. Rev.*, 2012, **112**, 869.
18 K. Sumida, D. L. Rogow, J. A. Mason, J. R. Long, *et al.*, *Chem. Rev.*, 2012, **112**, 724.
19 Y. He, W. Zhou, G. Qian, B. Chen, *et al.*, *Chem. Soc. Rev.*, 2014, **43**, 5657.
20 Y. Peng, J. T. Hupp, O. K. Farha and T. Yildirim, *J. Am. Chem. Soc.*, 2013, **135**, 11887.
21 J. Jiang, H. Furukawa, Y.-B. Zhang and O. M. Yaghi, *J. Am. Chem. Soc.*, 2016, **138**, 10244.
22 S. Xiang, Y. He, Z. Zhang, R. Krishna, B. Chen, *et al.*, *Nat. Commun.*, 2012, **3**, 954.
23 S. Ma and H.-C. Zhou, *Chem. Commun.*, 2010, **46**, 44.
24 T. Islamoglu, S. Goswami, O. K. Farha and J. T. Hupp, *Acc. Chem. Res.*, 2017, **50**, 805.
25 K. Adil, Y. Belmabkhout, M. Eddaoudi, *et al.*, *Chem. Soc. Rev.*, 2017, **46**, 3402.
26 Z. Bao, G. Chang, H. Xing, R. Krishna, Q. Ren, B. Chen, *et al.*, *Energy Environ. Sci.*, 2016, **9**, 3612.
27 E. D. Bloch, W. L. Queen, R. Krishna, J. M. Zadrozny, C. M. Brown and J. R. Long, *Science*, 2012, **335**, 1606.
28 R.-B. Lin, L. Li, H.-L. Zhou, H. Wu, C. He, J. Li, W. Zhou, B. Chen, *et al.*, *Nat. Mater.*, 2018, **17**, 1128.
29 Z. R. Herm, E. D. Bloch and J. R. Long, *Chem. Mater.*, 2014, **26**, 323.
30 S. J. Gerier, J. A. Mason, E. D. Bloch, W. L. Queen, M. R. Hudson, C. M. Brown and J. R. Long, *Chem. Sci.*, 2013, **4**, 2054.
31 Y. He, R. Krishna and B. Chen, *Energy Environ. Sci.*, 2012, **5**, 9107.
32 V. F. D. Martins, A. M. Ribeiro, A. E. Rodrigues, *et al.*, *Sep. Purif. Technol.*, 2015, **149**, 445.
33 D. J. Safarik and R. B. Eldridge, *Ind. Eng. Chem. Res.*, 1998, **37**, 2571.
34 G. Chang, Z. Bao, Q. Ren, S. Deng, Z. Zhang, B. Su, H. Xing and Y. Yang, *RSC Adv.*, 2014, **4**, 20230.
35 F. Gao, Y. Wang, X. Wang and S. Wang, *Adsorption*, 2016, **22**, 1013.
36 G. Chang, Y. Su, Q. Ren, Z. Bao, B. Chen, *et al.*, *Chem. Commun.*, 2015, **51**, 2859.
37 B. Li, Y. Zhang, R. Krishna, K. Yao, Y. Han, Z. Wu, D. Ma, Z. Shi, S. Ma, *et al.*, *J. Am. Chem. Soc.*, 2014, **136**, 8654.
38 Y. Zhang, B. Li, R. Krishna, Z. Wu, D. Ma, Z. Shi, S. Ma, *et al.*, *Chem. Commun.*, 2015, **51**, 2714.
39 Y. Wang, Z. Hu, Y. Cheng and D. Zhao, *Ind. Eng. Chem. Res.*, 2017, **56**, 4508.
40 U. Böhme, B. Barth, C. Paula, A. Kuhnt, W. Schwieger, J. Caro and M. Hartmann, *Langmuir*, 2013, **29**, 8592.
41 W. Liang, F. Xu, X. Zhou, J. Xiao, Q. Xia, Y. Li and Z. Li, *Chem. Eng. Sci.*, 2016, **148**, 275.
42 P.-Q. Liao, W.-X. Zhang, J.-P. Zhang and X.-M. Chen, *Nat. Commun.*, 2015, **6**, 8697.
43 Y. Chen, Z. Qiao, H. Wu, D. Lv, R. Shi, Q. Xia, J. Zhou and Z. Li, *Chem. Eng. Sci.*, 2018, **175**, 110.
44 R.-B. Lin, H. Wu, W. Zhou and B. Chen, *J. Am. Chem. Soc.*, 2018, **140**, 12940.
45 L. Li, R.-B. Lin, R. Krishna, H. Li, J. Li, B. Chen, *et al.*, *Science*, 2018, **362**, 443.
46 Y. Wu, H. Chen, D. Liu, Y. Qian and H. Xi, *Chem. Eng. Sci.*, 2015, **124**, 144.
47 N. Nijem, J.-F. Veyan, L. Kong, K. Li, J. Li, D. Langreth, Y. J. Chabal, *et al.*, *J. Am. Chem. Soc.*, 2010, **132**, 1654.
48 K. Tan, N. Nijem, P. Canepa, Q. Gong, J. Li, T. Thonhauser and Y. J. Chabal, *Chem. Mater.*, 2012, **24**, 3153.
49 A. Hijazi, J. C. Kemmegne-Mbouguen, E. Cadot, *et al.*, *Dalton Trans.*, 2013, **42**, 4848.
50 J. Pires, M. L. Pinto and V. K. Saini, *ACS Appl. Mater. Interfaces*, 2014, **6**, 12093.
51 Q. M. Wang, D. Shen, M. Bülow, M. L. Lau, S. Deng, F. R. Fitch, N. O. Lemcoff and J. Semanscin, *Microporous Mesoporous Mater.*, 2002, **55**, 217.
52 S. Yang, A. J. Ramirez-Cuesta, R. Newby, V. Garcia-Sakai, P. Manuel, M. Schröder, *et al.*, *Nat. Chem.*, 2015, **7**, 121.